Photonic Generation of Precisely π Phase-Shifted Binary Phase-Coded Microwave Signal

Ming Li, *Member, IEEE*, Ze Li, and Jianping Yao, *Fellow, IEEE*

***Abstract*— A novel photonic approach to generating a precisely π phase-shifted binary phase-coded microwave signal is proposed and experimentally demonstrated. A phase modulator is employed to generate two ±1st-order sidebands and an optical carrier. Due to the inherent $\pm\pi/2$ phase shifts of the two ±1st-order sidebands, a binary phase-coded microwave signal with a precise phase shift of π is generated through beating one sideband with the optical carrier at a time, which is realized by joint use of a polarization-maintaining fiber Bragg grating and a polarization modulator to select one of the two sidebands and the optical carrier. The generation of a binary phase-coded microwave signal with a precise π phase shift and with a tunable frequency from 18 to 22 GHz is experimentally demonstrated.**

***Index Terms*— Microwave phase coding, microwave photonics, microwave pulse compression, microwave signal generation, radar.**

I. Introduction

MICROWAVE pulse compression has been widely employed in modern radar systems to increase the range resolution [1]. Usually, microwave pulse compression is realized using a frequency-chirped or phase-coded pulse based on matched filtering in a radar receiver. In recent years, photonic generation of phase-coded microwave waveform has been widely investigated [2]–[9]. The advantages of photonic-assisted microwave waveform generation are the large bandwidth and high frequency which may not be achievable using the currently available electronic circuits. In [2], a phase-coded microwave pulse generated based on optical pulse shaping using a spatial light modulator (SLM) was proposed. The advantage of using an SLM is the high reconfigurability. However, the fiber-to-space and space-to-fiber coupling would make the system complicated and lossy. Recently, a phase-coded microwave pulse generated based on pure fiber optics was proposed, in which an optical electro-optic phase modulator (PM) was incorporated in one arm of a Mach–Zehnder interferometer (MZI) [6] or in a Sagnac interferometer (SI) [7] to perform phase coding. However, the systems in [6], [7] were sensitive to environmental perturbations due to the fact that the systems are interferometer based. More recently, phase-coded microwave waveform generated using a single polarization modulator (PolM) was demonstrated [8]. Compared with the techniques in [6], [7], the system is simpler. The major limitation of the technique in [8] is that the carrier frequency of the generated phase-coded microwave waveform is fixed with no tunability. Very recently, a technique similar to the one in [8] but with large tunability was proposed. A phase-coded microwave signal with a large tunable microwave frequency by using a polarization-maintaining fiber Bragg grating (PM-FBG) was demonstrated [9]. The phase-coded microwave signal generation is implemented by modulating two polarization-orthogonal sidebands at a PolM. The coded phase shift is tunable by changing the power of the modulation signal. The limitation of the technique is that the power of the modulation signal must be precisely controlled to ensure an accurate phase shift.

Recently, we have proposed and demonstrated a novel approach to generating a precisely π phase-shifted binary phase-coded microwave pulse, and some preliminary results have been obtained [10]. Here in this letter, a more detailed discussion and more experimental results will be presented.

It is different from the technique in [9], where the amount of phase shift is determined by the power of the modulation signal, here in this letter the phase shift, which is π, is determined by the inherent $\pm\pi/2$ phase shifts of the two 1^{st}-order sidebands of a phase-modulated signal. In addition to the precise π phase shift, the proposed technique has other two key features. First, since no interferometer is employed in the system, an ultra-stable operation is guaranteed. Second, the frequency tunable range is only determined by the bandwidth of the PM-FBG, which can be tens of GHz, thus large frequency tunability can be achieved. The proposed technique is experimentally demonstrated. The generation of a binary phase-coded microwave signal with a precise π phase shift and with a tunable frequency from 18 to 22 GHz is experimentally demonstrated. The pulse compression capability of the generated phased-coded pulses is also evaluated.

II. Principle

The schematic of the proposed binary phase-coded microwave signal generation system is shown in Fig. 1. A continuous-wave (CW) light wave from a tunable laser source (TLS) is sent to a PM which is driven by a microwave signal from a microwave signal generator (MSG) with a frequency of f_m. A programmable optical filter (POF) connected after the PM is used to filter out the sidebands higher than the $\pm 1^{st}$ order. In addition, the optical carrier is also attenuated to make its magnitude identical to the one of

Manuscript received June 5, 2012; revised August 13, 2012; accepted September 3, 2012. Date of publication September 24, 2012; date of current version October 31, 2012. This work was supported by the Natural Sciences and Engineering Research Council of Canada (NSERC).

The authors are with the Microwave Photonics Research Laboratory, School of Electrical Engineering and Computer Science, University of Ottawa, Ottawa, ON K1N 6N5, Canada (e-mail: jpyao@eecs.uottawa.ca).

Color versions of one or more of the figures in this letter are available online at http://ieeexplore.ieee.org.

Digital Object Identifier 10.1109/LPT.2012.2217486

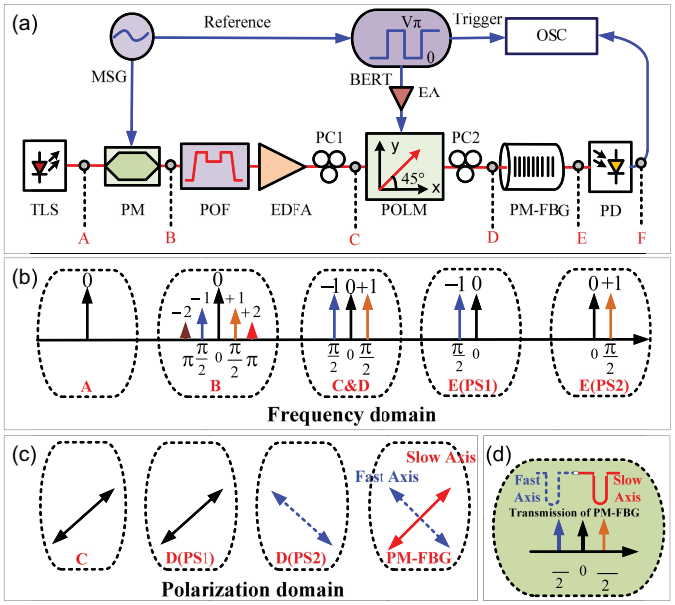

Fig. 1. (a) Schematic of the proposed binary phase-coded microwave signal generation system. Illustration of the operation principle: (b) frequency domain and (c) polarization domain. (d) Function of the PM-FBG to attenuate one sideband at a time. TLS: tunable laser. PM: electro-optic phase modulator. MSG: microwave signal generator. POF: programmable optical filter. EDFA: erbium-doped fiber amplifier. PC: polarization controller. POLM: polarization modulator. BERT: bit error rate tester. EA: electrical amplifier. PM-FBG: polarization maintaining fiber Bragg grating. PS: polarization state. PD: photodetector. OSC: oscilloscope.

the $\pm 1^{\text{st}}$-order sidebands. The optical wave at the output of the POF is amplified with an erbium-doped fiber amplifier (EDFA). The amplified signal is then sent to a PolM through a polarization controller (PC1). The output signal from the PolM is directed into a PM-FBG through a second PC (PC2). Due to the birefringence in the polarization-maintaining fiber (PMF), the PM-FBG has two orthogonally polarized and spectrally separated transmission bands. Fig. 1(b) and (c) shows the operation principle of the system in the frequency domain and in the polarization domain. The function of the PM-FBG for the selection of one sideband and the optical carrier is shown in Fig. 1(d).

As shown in Fig. 1(c), PC1 and PC2 are first adjusted to make the polarization direction of the incident light wave aligned with one principle axis of the PM-FBG (e.g., the slow axis). The $+1^{\text{st}}$-order sideband is suppressed by the PM-FBG. By beating the optical carrier and the -1^{st}-order sideband at a photodetector (PD), as shown in Fig. 1(d), a microwave signal at the frequency of the microwave drive signal is generated. There is an inherent phase offset between the -1^{st}-order sideband and optical carrier for a phase-modulated optical signal. The beating process would translate the phase offset into the generated microwave waveform.

Mathematically, under a small-signal modulation condition, the electrical field of a phase-modulated optical signal can be expressed as [11]

$$e_{PM}(t) = e_0\left\{J_0\cos(\omega_0 t) + J_1\cos\left[(\omega_0+\omega_m)t+\frac{\pi}{2}\right] + J_{-1}\cos\left[(\omega_0-\omega_m)t-\frac{\pi}{2}\right]\right\} \quad (1)$$

where e_0 and ω_0 are the amplitude and the angular frequency of the optical carrier, ω_m is the angular frequency of the microwave modulating signal, and $J_n(\cdot)$ denotes the nth-order Bessel function of the first kind.

Based on the Bessel function property, we have

$$J_{-1}(\cdot) = -J_1(\cdot). \quad (2)$$

Based on (2), (1) can be rewritten as

$$e_{PM}(t) = e_0\left\{J_0\cos(\omega_0 t) + J_1\cos\left[(\omega_0+\omega_m)t+\frac{\pi}{2}\right] - J_1\cos\left[(\omega_0-\omega_m)t-\frac{\pi}{2}\right]\right\}. \quad (3)$$

When the optical carrier and the $+1^{\text{st}}$-order sideband signal are directed into a PD, the signal at the output of the PD is given by

$$\begin{aligned} I_{PD1}(t) &= Re_0^2\left|J_0\cos(\omega_0 t) + J_1\cos\left[(\omega_0+\omega_m)t+\frac{\pi}{2}\right]\right|^2 \\ &= Re_0^2\left\{\frac{J_0^2}{2}[1+\cos(2\omega_0 t)] + \frac{J_1^2}{2}\{1+\cos[2(\omega_0+\omega_m)t+\pi]\} + 2J_0J_1\cos(\omega_0 t)\cos\left[(\omega_0+\omega_m)t+\frac{\pi}{2}\right]\right\} \end{aligned} \quad (4)$$

where R is the responsivity of the PD. Considering the limited bandwidth of the PD, the microwave current at the output of the PD is given by

$$I_{RF1}(t) = Re_0^2 J_0 J_1\cos\left(\omega_m t+\frac{\pi}{2}\right). \quad (5)$$

On the other hand, when the optical carrier and the -1^{st}-order sideband signal are launched into a PD, the signal at the output of the PD is given by

$$\begin{aligned} I_{PD2}(t) &= Re_0^2\left|J_0\cos(\omega_0 t) - J_1\cos\left[(\omega_0-\omega_m)t-\frac{\pi}{2}\right]\right|^2 \\ &= Re_0^2\left\{\frac{J_0^2}{2}[1+\cos(2\omega_0 t)] + \frac{J_1^2}{2}\{1+\cos[2(\omega_0-\omega_m)t-\pi]\} - 2J_0J_1\cos(\omega_0 t)\cos\left[(\omega_0-\omega_m)t-\frac{\pi}{2}\right]\right\}. \end{aligned} \quad (6)$$

Again, considering the limited bandwidth of the PD, the microwave current at the output of the PD is given by

$$\begin{aligned} I_{RF2}(t) &= -Re_0^2 J_0 J_1\cos\left(\omega_m t+\frac{\pi}{2}\right) \\ &= Re_0^2 J_0 J_1\cos\left(\omega_m t-\frac{\pi}{2}\right). \end{aligned} \quad (7)$$

It can be seen from (7) that the phase offset of the -1^{st}-order sideband related to the optical carrier is $-\pi/2$, and that of the $+1^{\text{st}}$-order sideband related to the optical carrier is $+\pi/2$, as shown in (5). By beating the optical carrier with the -1^{st}-order

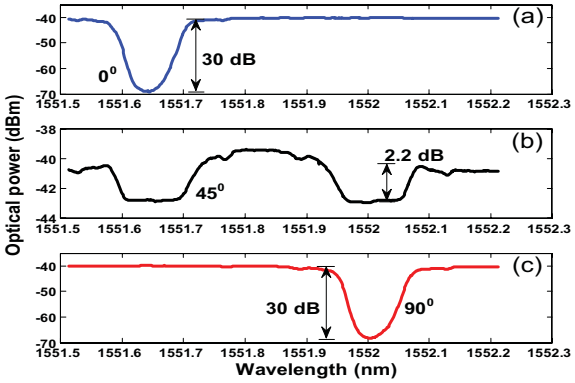

Fig. 2. Transmission spectra of the PM-FBG measured by a broadband light source with its polarization direction oriented at an angle of (a) 0°, (b) 45°, and (c) 90° to the fast axis of the PM-FBG.

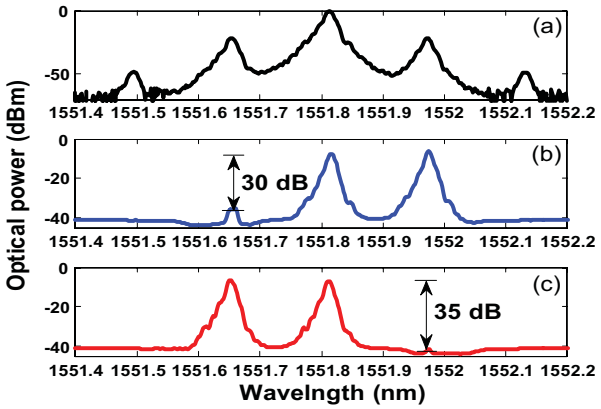

Fig. 3. (a) Optical spectrum measured at the output of the PM, which is driven by a microwave signal with a frequency of 22 GHz. Optical spectra measured at the output of the PM-FBG when the polarization direction is oriented at an angle of (b) 0° and (c) 90° to the fast axis of the PM-FBG.

sideband or the $+1^{st}$-order sideband at the PD, a microwave waveform with a phase of $-\pi/2$ or $+\pi/2$ is generated.

In the proposed system, the PolM is driven by a square wave with a low voltage of zero and a high voltage of V_π. When the input voltage applied to the PolM is zero, the $+1^{st}$-order sideband is suppressed, a microwave signal is then generated by beating the optical carrier with the $+1^{st}$-order sideband at the PD with an initial phase of $-\pi/2$. When the input voltage applied to the PolM is V_π, the polarization direction of the incident optical wave to the PMF-FBG will be rotated by 90°, and thus the -1^{st}-order sideband is suppressed. A microwave signal is then generated by beating the optical carrier with the $+1^{st}$-order sideband at the PD with an initial phase of $\pi/2$. Therefore, when the PolM is driven by the square waveform to switch the phase offset of the generated microwave waveform from $-\pi/2$ to $\pi/2$, a precise π phase shift is then coded into the microwave signal.

The key significance of this approach compared with the approaches reported in [8] and [9] is that the phase shift here is exactly π, which ensures better pulse compression performance compared with the approaches in [8], [9] where the phase shift is a function of the amplitude of the applied encoding signal.

III. Experiment

The proposed approach is experimentally evaluated. Fig. 2(a), (b) and (c) shows the transmission spectra of the PM-FBG measured using a broadband light source with its polarization direction aligned at an angle of 0°, 45° and 90° with respect to the fast axis of the PM-FBG, respectively. The wavelength spacing between the two transmission bands is about 0.36 nm. As shown in Fig. 2(a) and (c), the notch depth of the PMF-FBG corresponding to the slow axis and fast axis is larger than 30 dB, which is used to suppress one sideband for generating a phase-coded microwave signal by beating the other sideband with the optical carrier.

Fig. 3(a) shows the optical spectrum of the signal at the output of the PM which is driven by a microwave signal with a frequency of 22 GHz. Fig. 3(b) and (c) shows the optical spectra measured at the output of the PM-FBG when the polarization direction is oriented at an angle of 0° and 90° to the fast axis of the PM-FBG. A large isolation between the suppressed optical sideband and the other two spectral components of about 30 dB is achieved. To demonstrate the phase-coding capability, a 22-GHz binary phase-coded microwave signal is first generated. The phase-coding signal is a 5.5-Gb/s "0101" digital sequence from a Bit Error-Rate tester (BERT) (Agilent N4901B). Fig. 4(a) shows the phase-coded microwave signal and Fig. 4(b) shows the phase information recovered from the phase-coded signal using the Hilbert transform. As can be seen, the phase shift is 180°, which agrees well with the theoretical value.

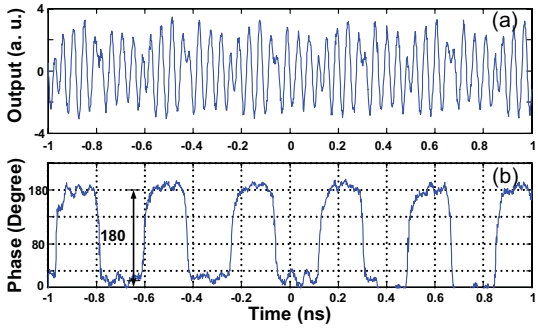

Fig. 4. (a) Generated 22-GHz binary phase-coded signal. (b) Recovered phase information from the binary phase coded microwave signal in (a).

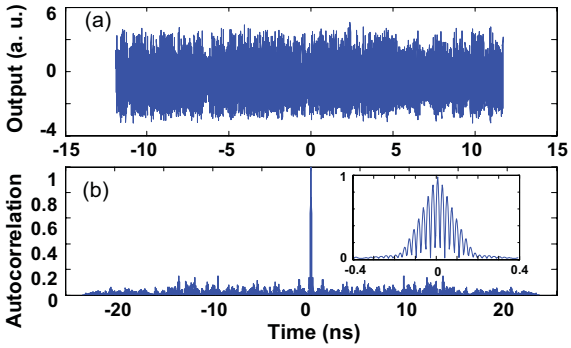

Fig. 5. (a) Binary phase-coded signals and (b) calculated autocorrelation of the signal with a carrier frequency of 22 GHz.

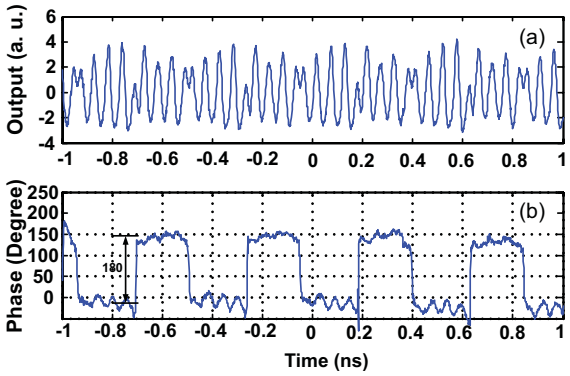

Fig. 6. (a) Generated 18-GHz binary phase-coded signal. (b) Recovered phase information from the binary phase-coded microwave signal in (a).

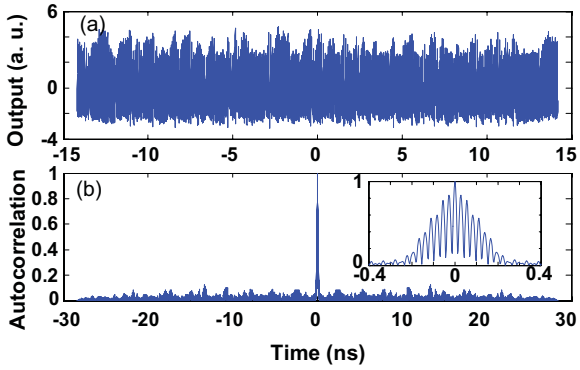

Fig. 7. (a) Binary phase-coded signals and (b) calculated autocorrelation of the signal with a carrier frequency of 18 GHz.

To demonstrate the pulse compression capability, a second phase-coded signal at 22 GHz is generated. This time, the phase-coding signal is also a 5.5-Gb/s pseudo-random bit sequence (PRBS), but with a length of 128 bits. Fig. 5(a) shows the generated 22-GHz phase-coded signal with a time duration of 23.27 ns. Fig. 5(b) shows the autocorrelation of the binary phase-coded microwave signal. A significantly compressed pulse is obtained. The autocorrelation peak has a full width at half-maximum (FWHM) of about 0.18 ns, and the compression ratio is about 129.28. The peak-to-sidelobe ratio (PSR) in Fig. 5(b) is about 8.3, which is much larger than those in [7] and [8] thanks to the accurate π phase shift in the phase-coded pulse.

Finally, the frequency tunability of the phase-coded microwave signal is evaluated. To do so, we tune the frequency of the microwave drive signal. As can be seen from Fig. 6(a), a binary phase-coded microwave signal at 18 GHz is generated. Fig. 6(b) shows the phase information recovered from the phase-coded signal which is also a 4.5-Gb/s "0101" digital sequence. Again, a π phase shift is achieved. The pulse compression capability at this new frequency is also evaluated. The phase-coding signal is a 4.5-Gb/s PRBS with a length of 128 bits. Fig. 7(a) shows the generated 18-GHz phase-coded signal with a time duration of 28.44 ns. Fig. 7(b) shows the autocorrelation. The autocorrelation peak has an FWHM of about 0.22 ns. The compression ratio is about 126.96 and the PSR is about 8.2.

Note that, the frequency tunable range here is from 18 to 22 GHz. As shown in Figs. 2 and 3, the tunable range is determined by the bandwidths of the FBGs in the two axes and the wavelength spacing between the FBGs. To increase the tunable range, the strength of the FBGs can be increased to achieve broader bandwidths. Also, a PMF with a higher refractive index difference can be used to increase the wavelength spacing between the FBGs.

IV. Conclusion

We have proposed and experimentally demonstrated a novel photonic approach to generating a binary phase-coded microwave signal with a precise π phase shift. Since the two 1st-order sidebands of a phase-modulated signal has an inherent π phase difference, the beating between one sideband and the optical carrier will have an exact π phase difference compared with the beating between the other sideband with the optical carrier. The key component in the system is the PM-FBG, which could select one sideband and the optical carrier with the help of the PolM. Since the bandwidth of a PM-FBG can be as large as tens of GHz, large carrier frequency tunability can be achieved. The generation of a binary phase-coded microwave signal with a tunable frequency at 18 and at 22 GHz was experimentally demonstrated. The pulse compression ratio and the PSR at 18 GHz were 126.96 and 8.2, and at 22 GHz were 129.28 and 8.3. The proposed approach is particularly suitable for applications where an exact π phase shift is needed.

References

[1] M. I. Skolnik, *Introduction to Radar*. New York: McGraw-Hill, 1962.
[2] J. Chou, Y. Han, and B. Jalali, "Adaptive RF-photonic arbitrary waveform generator," *IEEE Photon. Technol. Lett.*, vol. 15, no. 4, pp. 581–583, Apr. 2003.
[3] J. D. McKinney, D. E. Leaird, and A. M. Weiner, "Millimeter-wave arbitrary waveform generation with a direct space-to-time pulse shaper," *Opt. Lett.*, vol. 27, no. 5, pp. 1345–1347, Aug. 2002.
[4] M. Khan, *et al.*, "Ultrabroad-bandwidth arbitrary radiofrequency waveform generation with a silicon photonic chip-based spectral shaper," *Nature Photon.*, vol. 4, pp. 117–122, Feb. 2010.
[5] P. Ghelfi, F. Scotti, F. Laghezza, and A. Bogoni, "Photonic generation of phase-modulated RF signals for pulse compression techniques in coherent radars," *J. Lightw. Technol.*, vol. 30, no. 11, pp. 1638–1644, Jun. 1, 2012.
[6] H. Chi and J. P. Yao, "An approach to photonic generation of high-frequency phase-coded RF pulses," *IEEE Photon. Technol. Lett.*, vol. 19, no. 10, pp. 768–770, May 15, 2007.
[7] Z. Li, W. Li, H. Chi, X. Zhang, and J. P. Yao, "Photonic generation of phase-coded microwave signal with large frequency tunability," *IEEE Photon. Technol. Lett.*, vol. 23, no. 11, pp. 712–714, Jun. 1, 2011.
[8] H. Chi and J. P. Yao, "Photonic generation of phase-coded millimeter-wave signal using a polarization modulator," *IEEE Microw. Wireless Compon. Lett.*, vol. 18, no. 5, pp. 371–373, May 2008.
[9] Z. Li, M. Li, H. Chi, X. Zhang, and J. P. Yao, "Photonic generation of phase-coded millimeter-wave signal with large frequency tunability using a polarization-maintaining fiber Bragg grating," *IEEE Microw. Wireless Compon. Lett.*, vol. 21, no. 12, pp. 694–696, Dec. 2011.
[10] M. Li, Z. Li, and J. P. Yao, "Optical generation of binary phase-coded microwave signal using a polarization-maintaining fiber Bragg grating," in *Proc. 2011 IEEE Photon. Conf.*, Oct., pp. 481–482.
[11] J. P. Yao, F. Zeng, and Q. Wang, "Photonic generation of ultrawideband signals," *J. Lightw. Technol.*, vol. 25, no. 11, pp. 3219–3235, Nov. 2007.